Thermodynamic analysis of a Liquid Air Energy Storage System

Giuseppe Leo Guizzi[a], Michele Manno[a,*], Ludovica Maria Tolomei[a], Ruggero Maria Vitali[a]

[a]*Dept. of Industrial Engineering, University of Rome Tor Vergata, Italy*

Abstract

The rapid increase in the share of electricity generation from renewable energy sources is having a profound impact on the power sector; one of the most relevant effects of this trend is the increased importance of energy storage systems, which can be used to smooth out peaks and troughs of production from renewable energy sources.

Besides their role in balancing the electric grid, energy storage systems may provide also several other useful services, such as price arbitrage, stabilizing conventional generation, etc.; therefore, it is not surprising that many research projects are under way in order to explore the potentials of new technologies for electric energy storage.

This paper presents a thermodynamic analysis of a cryogenic energy storage system, based on air liquefaction and storage in an insulated vessel. This technology is attractive thanks to its independence from geographical constraints and because it can be scaled up easily to grid-scale ratings, but it is affected by a low round-trip efficiency due to the energy intensive process of air liquefaction. The present work aims to assess the efficiency of such a system and to identify if and how it can achieve an acceptable round-trip efficiency (in the order of 50÷60%).

Keywords: Energy storage, Cryogenic energy storage, Liquid Air

*Corresponding author
Email address: michele.manno@uniroma2.it (Michele Manno)

Giuseppe Leo Guizzi, Michele Manno, Ludovica Maria Tolomei, Ruggero Maria Vitali, Thermodynamic analysis of a liquid air energy storage system, Energy 93 (2015) 1639-1647, https://doi.org/10.1016/j.energy.2015.10.030.

1. Introduction

In recent years, the share of total installed capacity covered by intermittent renewable sources has increased impressively in many developed and non-developed countries; for example, in Italy the installed capacity of wind and photovoltaic plants has risen from 6,0 GW up to 27,0 GW in the period 2009-2013, while peak demand on the national grid in the same period was fairly constant, at approximately $52 \div 54$ GW [1].

This trend has underlined the importance of developing new grid-scale electric energy storage technologies, which could greatly improve the value of renewable energy sources acting as a buffer balancing their intermittent generation [2]. Furthermore, besides the most obvious services of load levelling and peak shaving, electric energy storage plants can find other applications [2, 3], such as provision of balancing energy, spinning reserve, black-start services, price arbitrage, stabilization of conventional generation, island and off-grid storage, *etc.*, which are very important for electric grid management and can be another source of revenue for the storage plant [3].

At the moment, only two technologies can be considered mature for grid-scale energy storage [4, 5]: pumped hydro (PHES) and compressed air energy storage (CAES). These options, though, both present a considerable drawback: the plant's location is constrained by geological features (such as the availability of an underground cavern for CAES). In particular, it is difficult to foresee any significant increase in pumped hydro capacity, at least in developed countries, because the most attractive sites have already been used. For these reasons considerable effort has been devoted by researchers worldwide in order to devise different technological options for electric energy storage that could provide efficient, economical, geographically unconstrained and environmentally safe solutions [2, 4–8].

Among the innovative proposals for electric energy storage, cryogenic energy storage (CES) and in particular liquid air energy storage systems (LAES) hold great promise, because they rely on mature technologies developed for more established applications, such as the gas liquefaction industry, and are geographically unconstrained: energy is stored in a cryogenic fluid in liquid phase, thereby greatly reducing the volume of the reservoir needed in comparison to a more conventional CAES system.

A LAES pilot plant (350 kW/2.5 MWh) was developed in Scotland by the UK company Highview Power Storage [9], and a larger prototype plant (5 MW/15 MWh) is under construction in the UK [10]. The company and

Giuseppe Leo Guizzi, Michele Manno, Ludovica Maria Tolomei, Ruggero Maria Vitali, Thermodynamic analysis of a liquid air energy storage system, Energy 93 (2015) 1639-1647, https://doi.org/10.1016/j.energy.2015.10.030.

the researchers promoting this solution claim several advantages for LAES technology: high energy density; no geographical constraints; high storage capacity; low investment costs; long useful life; possibility of waste heat recovery from nearby industrial plants; no environmental hazards [11]. The expected performance of liquid air storage in terms of round-trip efficiency is in the range $50 \div 60\%$ [11], which may seem rather disappointing; however, the proponents of these plants observe that, as long as the overall storage capacity is smaller than the excess power generated by intermittent renewable energy sources, the round-trip efficiency has a smaller impact on the economic performance of the storage plant than the investment cost [11, 12].

A few studies on the overall round-trip performance of LAES plants with different configurations are available in the literature. Chino and Araki [13] proposed an air liquefaction plant integrated with a conventional combined cycle power plant: when on-peak power demands increase, the plant is operated in energy recovery mode, in which compressed air is supplied to the combustor of the gas turbine by a cryogenic pump, fed with the liquid air stored in an insulated tank, instead of the conventional air compressor. The plant achieves high efficiency in the liquefaction section thanks to the recovery of cold exergy from liquefied air, which is stored in a storage medium and later used in the liquefaction section (at off-peak hours, when the plant is operated in energy storage mode). The resulting round-trip efficiency is higher than 70%.

Ameel *et al.* considered a storage plant based on a liquid air Rankine cycle [14]. In this case a round-trip efficiency of only around 43% was demonstrated, but the proposed configuration was peculiar because it relied on an external supply of liquid air to be added to the liquid air produced within the plant, and there seemed to be no integration of heat/cold storage.

Li *et al.* studied a LAES system integrated with a nuclear power plant [15]. The heat input in the recovery section of the energy storage system was supplied by steam bled from the nuclear power plant, with a turbine inlet temperature of 280 °C; the recovery and the liquefaction section were thermodynamically coupled by means of a cold storage system, based on a pair of thermal fluids (propane and methanol) selected because of their comparatively large heat capacity. The system reached a round-trip efficiency higher than 70%, thanks to the tight integration between recovery and liquefaction sections, to a turbine configuration with three reheatings, and also to quite optimistic values of isentropic efficiencies and pinch-point temperature differences.

Giuseppe Leo Guizzi, Michele Manno, Ludovica Maria Tolomei, Ruggero Maria Vitali, Thermodynamic analysis of a liquid air energy storage system, Energy 93 (2015) 1639-1647, https://doi.org/10.1016/j.energy.2015.10.030.

In this paper a LAES system is studied, which shares some features on one hand with the plant proposed in [15] (with particular reference to the liquefaction and cold storage section), and on the other with an adiabatic CAES plant (heat recovery and storage from the intercooling of compressed air). This configuration, which is described in detail in the following section, allows to evaluate the performance of a stand-alone LAES system, i.e. a system that does not rely on any external heat input (such as waste heat from an industrial plant or heat derived from an adjacent power plant).

2. Plant layout

The layout of the proposed LAES plant is represented in fig. 1.

In the liquefaction island, air is first compressed to high pressure, in a two-step intercooled process where heat is recovered by a thermal oil which is then stored at relatively high temperatures in a hot storage section. Intermediate pressure ratios are selected in order to minimize compressor work, therefore achieving the maximum storage efficiency for a given overall pressure ratio. The thermal oil here considered is Essotherm 650, as modelled in the Media library of the Modelica software package [16].

The compressed air is then cooled in a cold box by means of the returning air from the air separator and by cold fluids stored in a Cold Storage section, before flowing in a cryoturbine; this expansion produces a vapour-liquid mixture that is collected and separated into a gas stream and a liquid stream in the air separator. The liquid air thus produced is stored in a tank, which effectively performs the most important storage function in this energy storage plant, at approximately 80 K and atmospheric pressure.

When the plant is operated in energy recovery mode, liquid air is pumped from its tank and heated up to near-ambient temperature by the cold fluids: in this way, it is possible to store liquefied air's cold exergy in the Cold Storage section, and reuse it later to liquefy air at very high efficiency. The cold fluids considered in this paper are the same as in [15], i.e. propane and methanol, given their high heat capacity, which reduces the storage volume required. This solution is preferred to storing cold energy in solid media such as pebbles or concrete [17, 18] because, as shown in [15] and by preliminary calculations by the authors as well, it requires a significantly smaller storage volume. In any case, it must be pointed out that this choice does not alter the thermodynamic process and, consequently, the plant's overall performance.

Giuseppe Leo Guizzi, Michele Manno, Ludovica Maria Tolomei, Ruggero Maria Vitali, Thermodynamic analysis of a liquid air energy storage system, Energy 93 (2015) 1639-1647, https://doi.org/10.1016/j.energy.2015.10.030.

The pumped air flows first in a regenerator, then in a superheater, where it is heated by the thermal oil stored in the Hot Storage section, and finally through a turbine. The expansion is divided in three steps with interheating, again accomplished by means of the thermal oil. Intermediate pressure ratios are chosen so as to maximize the turbine work output, therefore achieving the maximum recovery efficiency for a given overall expansion ratio. The thermal oil is returned to the Hot Storage section, where it is collected in an ambient-temperature tank, after having been cooled in the heat exchanger labelled as "heat rejection" in fig. 1. Indeed, this is essentially the only component in the plant where heat is rejected to the environment, since air is discharged from the regenerator at temperatures very close to ambient temperature.

The constitutive equations for the proposed plant were implemented and solved, for stationary operation, in Matlab. The thermodynamic properties of all fluids, with the exception of the thermal oil Essotherm 650, were evaluated by means of the REFPROP 9.1 software [19]. Ambient air was considered as a mixture of only nitrogen and oxygen, with mass fractions of 77% and 23% respectively; thermodynamic properties of nitrogen and oxygen are evaluated in REFPROP according to refs. [20] and [21] respectively.

3. Results and Discussion

3.1. Performance indicators

3.1.1. Round-trip efficiency and liquid air yield

The results of the simulations will be presented in this section mainly with reference to a few selected performance parameters, among which the most important is certainly the round-trip efficiency η_{RT}, simply defined as the work output in recovery mode divided by the work input in storage mode:

$$\eta_{RT} = \frac{W_{out}}{W_{in}} = \frac{m_{1R}\, w_T}{m_1\, w_C} \tag{1}$$

Here w_T and w_C represent the net specific work of the air turbine and compressor, respectively. For the power plant described in fig. 1, with a two-step compression and a three-step expansion, the net specific work output is calculated by means of energy conservation equations applied to each component (turbines and pump), where changes in kinetic and potential energy can be neglected with respect to changes in static enthalpy:

$$w_T = (h_{6R} - h_{7R}) + (h_{8R} - h_{9R}) + (h_{10R} - h_{11R}) - (h_{2R} - h_{1R}) \tag{2}$$

Giuseppe Leo Guizzi, Michele Manno, Ludovica Maria Tolomei, Ruggero Maria Vitali, Thermodynamic analysis of a liquid air energy storage system, Energy 93 (2015) 1639-1647, https://doi.org/10.1016/j.energy.2015.10.030.

with the last term accounting for the cryogenic pump operation, while the net specific work input is (again, neglecting kinetic energy changes):

$$w_C = (h_{2A} - h_1) + (h_{2C} - h_{2B}) - (h_4 - h_5) \tag{3}$$

where the last term accounts for the work produced by the cryoturbine.

Taking into account a full discharge of the energy storage system during the energy recovery mode, the total mass of liquid air flowing out of the liquid air tank (m_{1R}) must be equal to the total amount of liquid air (m_6) produced while operating in energy storage mode:

$$m_{1R} = m_6 = Y m_1 \tag{4}$$

In the above equation, the liquid yield Y has been introduced, which is the ratio of mass of liquid air produced to the mass of air aspirated by the compressor; the liquid air yield is a key performance parameter in any plant involving air liquefaction. In this case, therefore, the liquid air yield also corresponds to the ratio of liquid air fed to the energy recovery section and the total mass of air compressed in the liquefaction section:

$$Y = \frac{m_{1R}}{m_1} \tag{5}$$

Given this expression, the round-trip efficiency (eq. 1) can be rewritten in terms of liquid air yield:

$$\eta_{RT} = Y \frac{w_T}{w_C} \tag{6}$$

3.1.2. Exergy efficiencies

Other important indicators are the exergy efficiencies of the liquefaction and of the energy recovery section. In the proposed configuration, the exergy inputs for the storage section are the net specific work input ($m_1 w_C$) and the cold exergy provided by the cold fluids, while the exergy outputs are represented by the exergy associated to the amount of liquid air produced ($m_6 e_6$) and by the exergy content of the heat released to the thermal oil (Hot Storage). The cold exergy input can be evaluated as follows:

$$E_{CS} = m_{1C} (e_{2C} - e_{1C}) + m_{3C} (e_{4C} - e_{3C}) \tag{7}$$

while the hot exergy output is:

$$E_{HS} = m_{1H} (e_{1H} - e_{2H}) \tag{8}$$

Giuseppe Leo Guizzi, Michele Manno, Ludovica Maria Tolomei, Ruggero Maria Vitali, Thermodynamic analysis of a liquid air energy storage system, Energy 93 (2015) 1639-1647, https://doi.org/10.1016/j.energy.2015.10.030.

In the energy recovery operating mode, the exergy inputs are represented by the liquid air supply ($m_{1R}\, e_{1R}$) and by the hot exergy released by the thermal oil, which will be designated as E_{HR}; the exergy outputs are the specific work produced ($m_{1R}\, w_T$) and the cold exergy stored in the Cold Storage section, which is equal to E_{CS} as defined above in eq. 7. If the work done by circulation pumps in the hot storage circuits is neglected, the exergy associated to the heat input supplied by the thermal oil is:

$$E_{HR} = m_{3H}\,(e_{3H} - e_{2H}) = E_{HS} \tag{9}$$

It is clear that only a fraction of E_{HS}, corresponding to the exergy change $e_{3H} - e_{4H}$, is actually used in the recovery section, while the remaining heat is simply rejected to the environment (as pointed out above) because of the inefficiencies in the system.

Summing up all these contributions, the exergy efficiency for the energy storage section is defined as:

$$\eta_S = \frac{m_6 e_6 + E_{HS}}{m_1 w_C + E_{CS}} \tag{10}$$

while the exergy efficiency for the energy recovery section is:

$$\eta_R = \frac{m_{1R}\, w_T + E_{CS}}{m_{1R}\, e_{1R} + E_{HS}} \tag{11}$$

3.2. Optimum operating conditions

The default values of the most important design parameters considered in the simulation of the storage plant are given in table 1 (any missing parameter not included for brevity can be deduced from the results given in tables 2-4). Besides the values listed in this table, an important design choice is related to the maximum pressure both in the liquefaction and in the energy recovery section (pressures p_2 and p_{2R} respectively). It will be shown in what follows that for any set of design parameters (such as those listed in table 1), an optimum compression ratio p_2/p_1 exists for each pump outlet pressure p_{2R}, while the influence of different values of p_{2R} will be discussed later in section 3.4.

The results of simulations carried out holding the recovery pressure constant at $p_{2R} = 6.5\,\mathrm{MPa}$ are given in fig. 2, in terms of round-trip efficiency, exergy efficiency and liquid air yield; the compressed air temperature T_4 at the cold-box outlet is also represented.

Giuseppe Leo Guizzi, Michele Manno, Ludovica Maria Tolomei, Ruggero Maria Vitali, Thermodynamic analysis of a liquid air energy storage system, Energy 93 (2015) 1639-1647, https://doi.org/10.1016/j.energy.2015.10.030.

This graph clearly shows that, for relatively low values of p_2, an increase in compression ratio results in increasing values of liquid air yield and efficiency, until a maximum is reached when the liquid air yield Y remains almost constant and the efficiency starts decreasing. Temperature T_4 actually explains this behaviour: the maximum efficiency is reached when the pinch-point is located at the cold end of the heat exchanger, allowing the compressed air to reach a minimum temperature of 98 K with the parameters given in table 1. When this condition is reached, any further increase in pressure does not yield any benefit, because the corresponding increase in net work input is not balanced by a significant increase in liquid air yield, which is effectively held almost constant by the temperature profile of the cold fluids in the Cold Storage section once a pinch-point is reached at the cold end of the heat exchanger.

The optimum configuration can also be explained in terms of entropy generation minimization within the cold box, as illustrated by figs. 3-5, which represent the heat exchange diagrams for the Cold Box at different compression ratios. The heat flux represented in abscissae is normalized with reference to the mass flow rate of compressed air.

The energy balance for the cold box, with reference to a unit mass flow rate of compressed air, is:

$$Q_{CB} = Q_{cf} + Q_{ca} \tag{12}$$

where $Q_{CB} = h_2 - h_4$ is the heat flux released by the compressed air, $Q_{ca} = (1 - Y)(h_9 - h_7)$ is the heat flux absorbed by the cold air flowing out of the separator and Q_{cf} is the heat flux absorbed by the cold fluids, whose amount is defined by the energy recovery process:

$$Q_{cf} = m^*_{1C}\,(h_{2C} - h_{1C}) + m^*_{3C}\,(h_{4C} - h_{3C}) = Y\,(h_{4R} - h_{2R}) \tag{13}$$

and is therefore dependent only on the liquid air yield Y and on maximum pressure p_{2R} in the energy recovery section (here m^* denote the cold fluid mass flow rate divided by the mass flow rate of compressed air).

It is well known that, in general, in order to increase the liquid air yield in any liquefaction plant it is necessary to increase the compression ratio [22]. Taking this into account, it follows that for relatively small compression ratios (fig. 3), the liquid air yield is also comparatively small: this will lead to a relatively small amount of cold energy stored in the Cold Storage section, because the mass of liquid air available for the energy recovery process is

Giuseppe Leo Guizzi, Michele Manno, Ludovica Maria Tolomei, Ruggero Maria Vitali, Thermodynamic analysis of a liquid air energy storage system, Energy 93 (2015) 1639-1647, https://doi.org/10.1016/j.energy.2015.10.030.

equal to the liquid air yield. Therefore, the cold air in the cold box absorbs a relatively large heat flux (eq. 12) so that its temperature increase is quite steep: for this reason, the pinch-point in the heat exchanger is located close to the hot end of the second heat exchanger and is dictated by the temperature difference between compressed air and cold air.

As the compression ratio increases, the liquid air yield also increases, and the slope of the curve corresponding to the cold air decreases: therefore, the compressed air curve shifts downwards, its outlet temperature (T_4) decreases and the distance between compressed air and cold fluids in the heat exchange diagram also decreases. Overall, this leads to higher efficiencies, until the temperature difference at the cold end between compressed air and cold fluid is exactly equal to the minimum temperature difference allowed: the minimum possible temperature T_4 is reached at this point, as described in fig. 4, which clearly shows two pinch-points in the cold-box: in this configuration the entropy generation within the cold box is clearly minimized since the distance between the fluids is the minimum possible given the design constraints.

Finally, if the compression ratio is further increased (fig. 5), the performance of the systems is reduced for several reasons:

- the increase in liquid air yield is negligible, because compressed air cannot be cooled further because of the location of the pinch-point at the cold end of the heat exchanger;
- the temperature drop for compressed air ($T_2 - T_4$) is now constant, but the corresponding enthalpy change decreases because the Joule-Thomson coefficient is positive at point 2 while negative at point 4 (so that h_2 decreases and at the same time h_4 increases), and this explains the reduction in overall heat exchange between fig. 4 and fig. 5;
- the amount of cooling provided by the cold fluids in the cold box is almost constant (eq. 13);
- as a result, the cold air flowing out of the separator receives less heat than in the optimum configuration, thus its curve in the heat exchange diagram shifts downward moving away from the compressed air curve, leading to higher inefficiency.

Giuseppe Leo Guizzi, Michele Manno, Ludovica Maria Tolomei, Ruggero Maria Vitali, Thermodynamic analysis of a liquid air energy storage system, Energy 93 (2015) 1639-1647, https://doi.org/10.1016/j.energy.2015.10.030.

3.3. Results for the reference configuration

In this section, the results of the simulation for a reference configuration are given; the reference configuration is defined by the design parameters given in table 1 and by a recovery pressure $p_{2R} = 6.5\,\text{MPa}$. The corresponding optimum compression ratio is found to be $p_2/p_1 = 179.2$, which results in a round-trip efficiency of $\eta_{RT} = 54.4\%$ (see fig. 2).

An important consideration to be made is related to the very high pressure required in the liquefaction section in order to optimize the overall performance (high compression ratios provide both high liquid air yields and large quantities of heat storage). Compression ratios in the order of $150 \div 200$ for air are certainly not impossible to reach, and require a commercially-proven technology such as multistage vertically-split centrifugal compressors. More critical may be such a high expansion ratio for the cryoturbine; these components are widely used in the natural gas liquefaction industry, and high isentropic efficiencies have been claimed [15], but this technology probably cannot be considered as mature as that required by the compressor.

The stream data resulting from the simulation are listed in table 2 for the liquefaction section, in table 3 for the energy recovery section (here t_R is the operational period in energy recovery and t_S is the operational period in storage mode) and finally in table 4 for cold fluids and thermal oil; the thermodynamic diagrams for the liquefaction and recovery sections are given in figs. 6-7 and the heat exchange diagram for the first intercooler in the storage section is shown in fig. 8.

It is of particular importance to point out the density of air in the storage tank (point 6 in table 2), which is more than six times higher than the density of air stored at 120 bar and ambient temperature [19]: since the net work outputs of a LAES and of an adiabatic CAES system are comparable, this characteristic makes the former much less demanding in terms of storage volume required.

More specifically, the net work output in this reference configuration is $w_T = 428.3\,\text{kJ/kg}$ (eq. 2): taking into account a reduction of round-trip efficiency down to approximately 50%, due to pressure drops, discharge losses in thermal energy storage, auxiliary consumption and so on, an effective value of $w_{T,eff} \approx 390\,\text{kJ/kg}$ can be expected. This means that, taking this value as the average during a complete energy recovery cycle, in order to recover a significant amount of electric energy such as $E = 500\,\text{MWh}$ the mass of liquid air that needs to be produced and stored is $m_a = E/w_{T,eff} = 4615\,\text{t}$. The storage volume required (of liquid air only) is therefore $V_a = m_a/\rho_6 \approx$

Giuseppe Leo Guizzi, Michele Manno, Ludovica Maria Tolomei, Ruggero Maria Vitali, Thermodynamic analysis of a liquid air energy storage system, Energy 93 (2015) 1639-1647, https://doi.org/10.1016/j.energy.2015.10.030.

5300 m^3, one order of magnitude lower than that required by a CAES system of the same rating. Even taking into account the storage volume required in the Hot Storage and Cold Storage sections, a LAES system has a considerably smaller footprint than an adiabatic CAES plant and therefore does not suffer the same limitations in terms of location of the storage plant.

The exergy analysis for the system is illustrated in figs. 9-11. In particular, fig. 9 gives an overview of exergy losses for the overall energy storage plant, where it is shown that exergy losses are approximately of the same order of magnitude in the storage (liquefaction) and in the energy recovery section, while the exergy loss associated to the heat rejected to the environment is the smallest contribution.

Figure 10 shows the exergy efficiency and the distribution of exergy losses of the storage section. The exergy efficiency for this part of the plant is very high, at 84.7%, thanks to the integration with the recovery section; the outputs are liquefied air (58.5%), produced with a yield $Y = 84.2\%$, and heat stored in the thermal oil (26.2%). Among the exergy losses, the largest contributions are related to the air compression process and to irreversibility in the Cold Box heat exchangers. In both cases, it is difficult to take into consideration significant improvements, because design parameters and configuration are already quite demanding.

Figure 11 illustrates the second-law analysis for the energy recovery section. Here, besides heat rejection, the largest exergy losses are again due to the irreversibility in the heat exchange between air and cold fluids and to the work exchange process (expansion in this case). It is worth mentioning here that the adoption of quasi-isothermal expanders, which have been lately the subject of several studies [23], could significantly increase work output and round-trip efficiency; indeed, some of these studies were focused on liquid nitrogen or liquid air as the working fluid in a quasi-isothermal expander [24–26]. However, these devices are volumetric expanders that are probably very difficult to scale up to the size required by a grid-scale energy storage system.

3.4. Influence of design parameters

Figures 12-14 show how round-trip efficiency η_{RT} and optimum compressor outlet pressure p_2 change with maximum pressure p_{2R} in the recovery section. Each figure further describes the influence on system's performance of a particular design parameter, namely, cryoturbine efficiency (fig. 12), pressure losses in heat exchangers (fig. 13), cold-box heat exchanger efficiency

Giuseppe Leo Guizzi, Michele Manno, Ludovica Maria Tolomei, Ruggero Maria Vitali, Thermodynamic analysis of a liquid air energy storage system, Energy 93 (2015) 1639-1647, https://doi.org/10.1016/j.energy.2015.10.030.

(fig. 14). In general, it is possible to observe that an increase in maximum pressure in the recovery section leads to a significant increase in round-trip efficiency (approximately $1 \div 2$ percentage points for a 10 bar increase in pressure), but, on the other hand, the optimum compressor outlet pressure also increases significantly: therefore, pressure p_{2R} should be chosen as the highest possible taking into account the feasibility of the corresponding optimum compressor pressure ratio. Setting a limit on pressure ratio of approximately 180, the resulting maximum pressure in the recovery section, for the default design parameters listed in table 1, is $p_{2R} = 6.5\,\mathrm{MPa}$ (fig. 12), which is the value chosen for the reference configuration discussed in the previous section.

The performance of the cryoturbine is very important for the overall energy storage system: as fig. 12 shows, an increase in its isentropic efficiency leads not only to significantly better round-trip efficiencies, but it reduces also the optimum compression ratio, since the thermodynamic cycle in the liquefaction section (fig. 6) is affected by this parameter. As already pointed out in section 3.3, cryoturbines have been developed for LNG industry with rated isentropic efficiency as high as 88% [15]; however, due to the particular nature of the expansion (two phase with very low vapour quality), in this paper a conservative estimate of 70% has been made for the reference configuration.

The influence of pressure losses in heat exchangers is illustrated in fig. 13: the analysis has been carried out applying an equal value of relative pressure loss to all heat exchangers present in the storage plant (both in the recovery and in the storage section). Clearly, larger pressure drops lead to lower round-trip efficiencies, and in particular a decrease of approximately 0.9% in round-trip efficiency is observed for an increase of 1% in relative pressure drop. On the other hand, the graph also shows that the optimum compression ratio is very marginally affected by pressure losses.

Due to the nature of the system under study, it is not surprising to find that heat exchanger efficiencies affect significantly the plant's overall performance. Fig. 14 shows in particular the effect of different pinch-point temperature differences at the cold box heat exchanger, which is clearly the most important heat exchanger in the plant, since it dictates the liquid air yield and the exergy efficiency of the storage section. The results point out that a decrease in the pinch-point temperature difference of 5 K leads to a drop in round-trip efficiency of 2.2%. Even though the optimal choice of the pinch-point temperature difference should be the result of a thermo-economic analysis, which is beyond the scope of the present work, probably strict re-

Giuseppe Leo Guizzi, Michele Manno, Ludovica Maria Tolomei, Ruggero Maria Vitali, Thermodynamic analysis of a liquid air energy storage system, Energy 93 (2015) 1639-1647, https://doi.org/10.1016/j.energy.2015.10.030.

quirements (5 K) on this parameter should be expected as the result of such analysis.

4. Conclusions

In this paper, a thermodynamic analysis of a liquid air energy storage (LAES) plant has been carried out, in order to assess if reasonable round-trip efficiencies can be obtained in a stand-alone configuration, i.e. with the heat input in the energy recovery section provided by heat stored during the air liquefaction process (as in the case of an adiabatic CAES system), rather than by any external heat source (for example, waste heat available from an industrial plant).

The results obtained have shown that a round-trip efficiency in the range $54 \div 55\%$ can indeed be obtained with reasonable and conservative design parameters and state-of-the-art technologies, so that, even taking into account auxiliary consumption, pressure drops in the power plant and self-discharge losses for thermal energy storage, a global efficiency of 50% can be considered within reach. This result is possible thanks to a tight integration between the storage and the recovery section of the plant, based on both cold and heat storage.

Among the many components of the storage plant, the most critical is the cryoturbine of the liquefaction section: in the proposed configuration, an isentropic efficiency of at least 70% is required in order to reach the round-trip efficiency target.

Therefore, a LAES system can probably be considered as a viable option for grid-scale (hundreds of MWh) electric energy storage, even in stand-alone configuration (but it would be even more suitable if a source of waste heat could be tapped), thanks to several positive features: besides its satisfactory efficiency, it is independent from geographical constraints, reliable, based on proven technologies and environmentally safe.

References

[1] Dati statistici sull'energia elettrica in italia. Tech. Rep.; Terna; 2013. URL: http://www.terna.it/default/Home/SISTEMA_ELETTRICO/statistiche/dati_statistici.aspx.

Giuseppe Leo Guizzi, Michele Manno, Ludovica Maria Tolomei, Ruggero Maria Vitali, Thermodynamic analysis of a liquid air energy storage system, Energy 93 (2015) 1639-1647, https://doi.org/10.1016/j.energy.2015.10.030.

[2] Ferreira HL, Garde R, Fulli G, Kling W, Lopes JP. Characterisation of electrical energy storage technologies. Energy 2013;53:288 –98. doi:10.1016/j.energy.2013.02.037.

[3] Peieper C, Rubel H. Revisiting energy storage. Tech. Rep.; The Boston Consulting Group; 2011.

[4] Evans A, Strezov V, Evans TJ. Assessment of utility energy storage options for increased renewable energy penetration. Renewable and Sustainable Energy Reviews 2012;16(6):4141–7. doi:10.1016/j.rser.2012.03.048.

[5] Rodrigues E, Godina R, Santos S, Bizuayehu A, Contreras J, Catalão J. Energy storage systems supporting increased penetration of renewables in islanded systems. Energy 2014;75:265 –80. doi:10.1016/j.energy.2014.07.072.

[6] Chen H, Cong T, Yang W, Tan C. Progress in electrical energy storage system: A critical review. Progress in Natural Science 2009;19(3):291–312. doi:10.1016/j.pnsc.2008.07.014.

[7] Ibrahim H, Ilinca A, Perron J. Energy storage systems—characteristics and comparisons. Renewable and Sustainable Energy Reviews 2008;12(5):1221 –50. doi:10.1016/j.rser.2007.01.023.

[8] Yekini Suberu M, Wazir Mustafa M, Bashir N. Energy storage systems for renewable energy power sector integration and mitigation of intermittency. Renewable and Sustainable Energy Reviews 2014;35:499–514. doi:10.1016/j.rser.2014.04.009.

[9] Energy storage – a revolution in the air. Modern Power Systems 2013;June:32–3. URL: http://viewer.zmags.com/publication/388070e3#/388070e3/32.

[10] GE storage agreement with Highview. Modern Power Systems 2014;April:4. URL: http://viewer.zmags.com/publication/f997bf2b#/f997bf2b/4.

[11] Liquid Air in the energy and transport systems. Tech. Rep.; The Centre for Low Carbon Futures; 2013. URL: http://bit.ly/liquid-air-full-report-2013.

Giuseppe Leo Guizzi, Michele Manno, Ludovica Maria Tolomei, Ruggero Maria Vitali, Thermodynamic analysis of a liquid air energy storage system, Energy 93 (2015) 1639-1647, https://doi.org/10.1016/j.energy.2015.10.030.

[12] Strbac G, Aunedi M, Pudjianto D, Djapic P, Teng F, Sturt A, et al. Strategic Assessment of the Role and Value of Energy Storage Systems in the UK Low Carbon Energy Future. Tech. Rep.; Energy Futures Lab, Imperial Conllege London; 2012. URL: http://bit.ly/strbac-2012.

[13] Chino K, Araki H. Evaluation of energy storage method using liquid air. Heat Transfer—Asian Research 2000;29(5):347–57. doi:10.1002/1523-1496(200007)29:5<347::AID-HTJ1>3.0.CO;2-A.

[14] Ameel B, T'Joen C, Kerpel KD. Thermodynamic analysis of energy storage with a liquid air Rankine cycle. Applied Thermal Engineering 2012;52(1):130–40. doi:10.1016/j.applthermaleng.2012.11.037.

[15] Li Y, Cao H, Wang S, Jin Y, Li D, Wang X, et al. Load shifting of nuclear power plants using cryogenic energy storage technology. Applied Energy 2014;113:1710–6. doi:10.1016/j.apenergy.2013.08.077.

[16] Modelica libraries. 2015. URL: https://www.modelica.org/libraries.

[17] Araki H, Nakabaru M, Chino K. Simulation of heat transfer in the cool storage unit of a liquid–air energy storage system. Heat Transfer—Asian Research 2002;31(4):284–96. doi:10.1002/htj.10035.

[18] Chai L, Liu J, Wang L, Yue L, Yang L, Sheng Y, et al. Cryogenic energy storage characteristics of a packed bed at different pressures. Applied Thermal Engineering 2014;63(1):439–46. doi:10.1016/j.applthermaleng.2013.11.030.

[19] Lemmon EW, Huber ML, McLinden MO. NIST Standard Reference Database 23: Reference Fluid Thermodynamic and Transport Properties - REFPROP, Version 9.1. National Institute of Standards and Technology, Standard Reference Data Program; Gaithersburg; 2013.

[20] Span R, Lemmon EW, Jacobsen RT, Wagner W, Yokozeki A. A Reference Equation of State for the Thermodynamic Properties of Nitrogen for Temperatures from 63.151 to 1000 K and Pressures to 2200 MPa. J Phys Chem Ref Data 2000;29(6):1361–433. doi:10.1063/1.1349047.

Giuseppe Leo Guizzi, Michele Manno, Ludovica Maria Tolomei, Ruggero Maria Vitali, Thermodynamic analysis of a liquid air energy storage system, Energy 93 (2015) 1639-1647, https://doi.org/10.1016/j.energy.2015.10.030.

[21] Schmidt R, Wagner W. A New Form of the Equation of State for Pure Substances and its Application to Oxygen. Fluid Phase Equilibria 1985;19:175–200. doi:10.1016/0378-3812(85)87016-3.

[22] Venkatarathnam G. Cryogenic Mixed Refrigerant Processes. Springer; 2008. ISBN 978-0-387-78513-4.

[23] Igobo ON, Davies PA. Review of low-temperature vapour power cycle engines with quasi-isothermal expansion. Energy 2014;70:22–34. doi:10.1016/j.energy.2014.03.123.

[24] Wen DS, Chen HS, Ding YL, Dearman P. Liquid nitrogen injection into water: Pressure build-up and heat transfer. Cryogenics 2006;46(10):740–8. doi:10.1016/j.cryogenics.2006.06.007.

[25] Clarke H, Martinez-Herasme A, Crookes R, Wen D. Experimental study of jet structure and pressurisation upon liquid nitrogen injection into water. International Journal of Multiphase Flow 2010;36(11-12):940–9. doi:10.1016/j.ijmultiphaseflow.2010.07.005.

[26] Chen H, Ding Y, Li Y, Zhang X, Tan C. Air fuelled zero emission road transportation: A comparative study. Applied Energy 2011;88(1):337–42. doi:10.1016/j.apenergy.2010.07.002.

Giuseppe Leo Guizzi, Michele Manno, Ludovica Maria Tolomei, Ruggero Maria Vitali, Thermodynamic analysis of a liquid air energy storage system, Energy 93 (2015) 1639-1647, https://doi.org/10.1016/j.energy.2015.10.030.

List of Tables

List of Figures

Giuseppe Leo Guizzi, Michele Manno, Ludovica Maria Tolomei, Ruggero Maria Vitali, Thermodynamic analysis of a liquid air energy storage system, Energy 93 (2015) 1639-1647, https://doi.org/10.1016/j.energy.2015.10.030.

Parameter	Value	units
Ambient temperature	25	°C
Ambient pressure	100	kPa
Liquid air storage pressure	100	kPa
Propane minimum temperature (T_{1C})	93	K
Propane maximum temperature (T_{2C})	214	K
Methanol minimum temperature (T_{3C})	214	K
Methanol maximum temperature (T_{4C})	288	K
Cold box HX pinch-point ΔT	5	K
Intercoolers pinch-point ΔT	10	K
Hot-end temperature approach at superheaters	10	K
Heat exchangers relative pressure loss	1%	
Isentropic efficiency of air turbines	0.85	
Isentropic efficiency of air compressors	0.85	
Isentropic efficiency of cryoturbine	0.70	
Isentropic efficiency of cryogenic pump	0.70	

Table 1: Default design parameters

Giuseppe Leo Guizzi, Michele Manno, Ludovica Maria Tolomei, Ruggero Maria Vitali, Thermodynamic analysis of a liquid air energy storage system, Energy 93 (2015) 1639-1647, https://doi.org/10.1016/j.energy.2015.10.030.

	$\frac{\dot{m}}{\dot{m}_1}$	p [MPa]	T [K]	h kJ/kg	ρ kg/m^3	N_2
1	1.000	0.100	296.24	299.50	1.17	79.5%
2A	1.000	1.480	687.74	707.454	7.40	79.5%
2B	1.000	1.465	308.15	308.727	16.48	79.5%
2C	1.000	18.098	682.00	705.204	85.32	79.5%
2	1.000	17.917	308.15	281.71	194.96	79.5%
3	1.000	17.738	245.80	198.70	261.28	79.5%
4	1.000	17.561	98.00	-77.38	825.80	79.5%
5	1.000	0.102	78.91	-93.87	28.17	93.0%
6	0.842	0.102	78.91	-126.21	871.26	77.0%
7	0.158	0.102	78.91	78.16	4.58	93.0%
8	0.158	0.101	237.80	244.26	1.45	93.0%
9	0.158	0.100	286.28	294.33	1.19	93.0%
10	0.842	0.100	298.15	300.47	1.16	77.0%

Table 2: Stream data in the liquefaction section for the reference configuration.

Giuseppe Leo Guizzi, Michele Manno, Ludovica Maria Tolomei, Ruggero Maria Vitali, Thermodynamic analysis of a liquid air energy storage system, Energy 93 (2015) 1639-1647, https://doi.org/10.1016/j.energy.2015.10.030.

	$\frac{\dot{m}}{\dot{m}_1}$	p [MPa]	T [K]	h kJ/kg	ρ kg/m^3	N_2
1R	0.842	0.100	78.74	-126.56	872.08	77.0%
2R	0.842	6.500	81.89	-116.13	873.20	77.0%
3R	0.842	6.435	209.00	180.44	120.39	77.0%
4R	0.842	6.371	283.00	269.84	79.56	77.0%
5R	0.842	6.307	436.27	436.35	49.13	77.0%
6R	0.842	6.244	616.42	628.96	34.27	77.0%
7R	0.842	1.590	450.55	454.68	12.18	77.0%
8R	0.842	1.574	616.42	628.96	8.80	77.0%
9R	0.842	0.401	451.23	456.27	3.08	77.0%
10R	0.842	0.397	616.42	629.01	2.23	77.0%
11R	0.842	0.101	451.42	456.69	0.78	77.0%
12R	0.842	0.100	288.00	290.19	1.20	77.0%

Table 3: Stream data in the recovery section for the reference configuration.

Giuseppe Leo Guizzi, Michele Manno, Ludovica Maria Tolomei, Ruggero Maria Vitali, Thermodynamic analysis of a liquid air energy storage system, Energy 93 (2015) 1639-1647, https://doi.org/10.1016/j.energy.2015.10.030.

	$\frac{\dot{m}}{\dot{m}_1}$	T [K]	h kJ/kg	fluid
1C	1.019	93.00	-182.18	propane
2C	1.019	214.00	62.72	propane
3C	0.437	214.00	-303.14	methanol
4C	0.437	288.00	-130.93	methanol
1H	0.999	626.42	849.94	thermal oil
2H	0.999	288.15	26.95	thermal oil
3H	0.999	626.42	849.94	thermal oil
4H	0.999	460.71	395.31	thermal oil

Table 4: Stream data (cold fluids and thermal oil) for the reference configuration.

Giuseppe Leo Guizzi, Michele Manno, Ludovica Maria Tolomei, Ruggero Maria Vitali, Thermodynamic analysis of a liquid air energy storage system, Energy 93 (2015) 1639-1647, https://doi.org/10.1016/j.energy.2015.10.030.

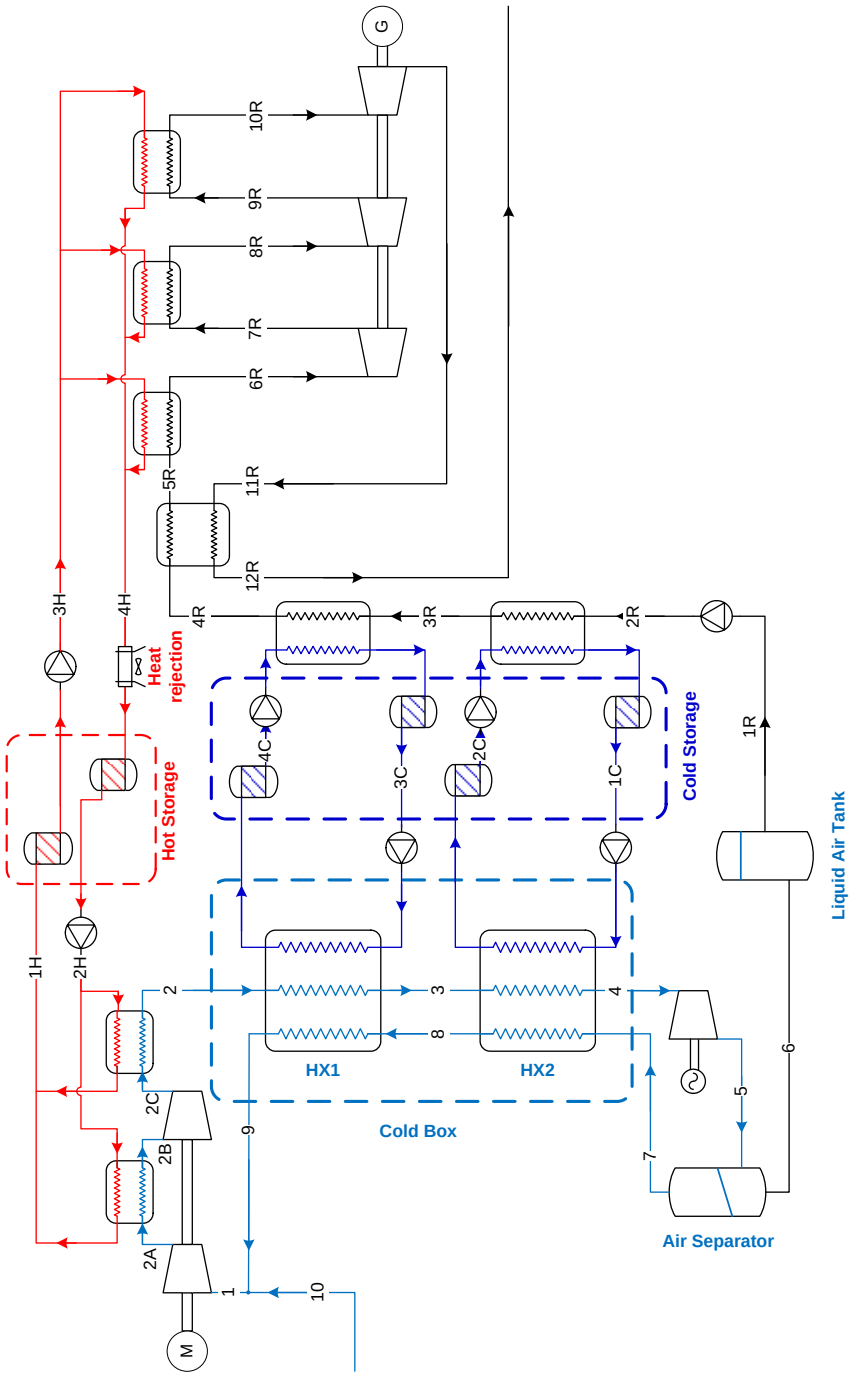

Figure 1: Proposed plant layout

Giuseppe Leo Guizzi, Michele Manno, Ludovica Maria Tolomei, Ruggero Maria Vitali, Thermodynamic analysis of a liquid air energy storage system, Energy 93 (2015) 1639-1647, https://doi.org/10.1016/j.energy.2015.10.030.

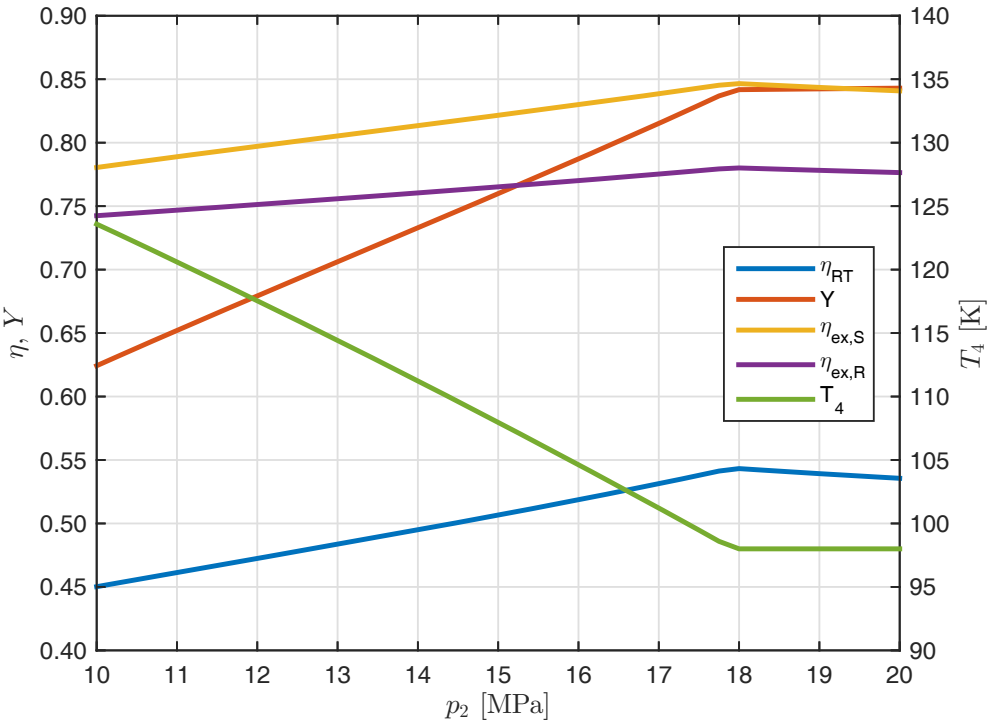

Figure 2: Round trip efficiency, exergy efficiencies, liquid air yield and compressed air temperature at cold-box outlet; maximum pressure in the energy recovery section $p_{2R} = 6.5\,\mathrm{MPa}$.

Giuseppe Leo Guizzi, Michele Manno, Ludovica Maria Tolomei, Ruggero Maria Vitali, Thermodynamic analysis of a liquid air energy storage system, Energy 93 (2015) 1639-1647, https://doi.org/10.1016/j.energy.2015.10.030.

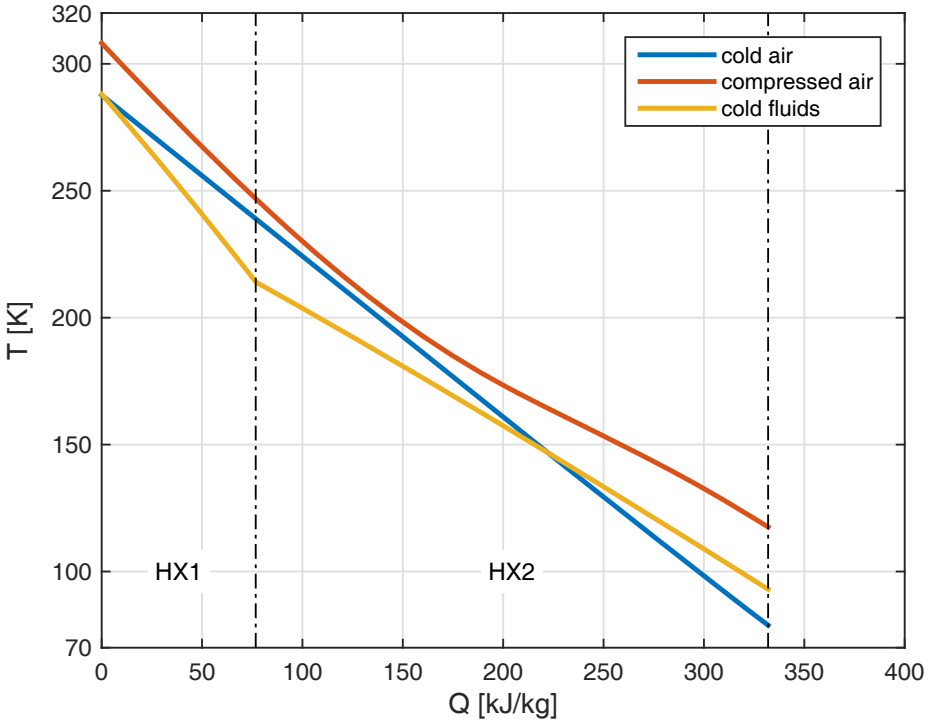

Figure 3: Cold Box heat exchange diagram for $p_{2R} = 6.5\,\mathrm{MPa}$ and $p_2 = 12.0\,\mathrm{MPa}$.

Giuseppe Leo Guizzi, Michele Manno, Ludovica Maria Tolomei, Ruggero Maria Vitali, Thermodynamic analysis of a liquid air energy storage system, Energy 93 (2015) 1639-1647, https://doi.org/10.1016/j.energy.2015.10.030.

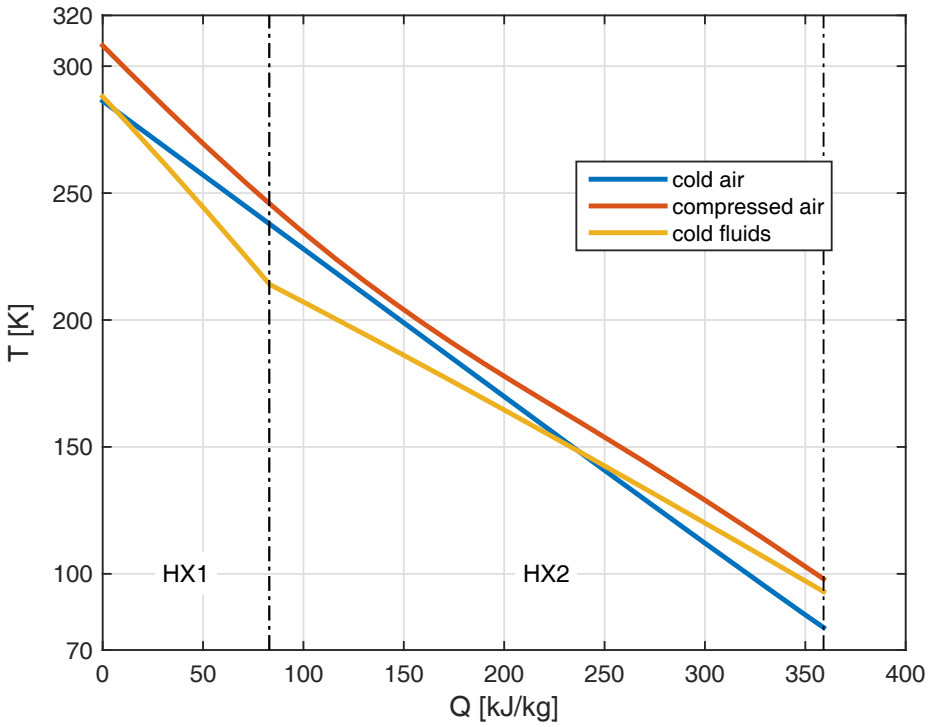

Figure 4: Cold Box heat exchange diagram for $p_{2R} = 6.5\,\mathrm{MPa}$ and $p_2 = 17.92\,\mathrm{MPa}$ (optimum configuration).

Giuseppe Leo Guizzi, Michele Manno, Ludovica Maria Tolomei, Ruggero Maria Vitali, Thermodynamic analysis of a liquid air energy storage system, Energy 93 (2015) 1639-1647, https://doi.org/10.1016/j.energy.2015.10.030.

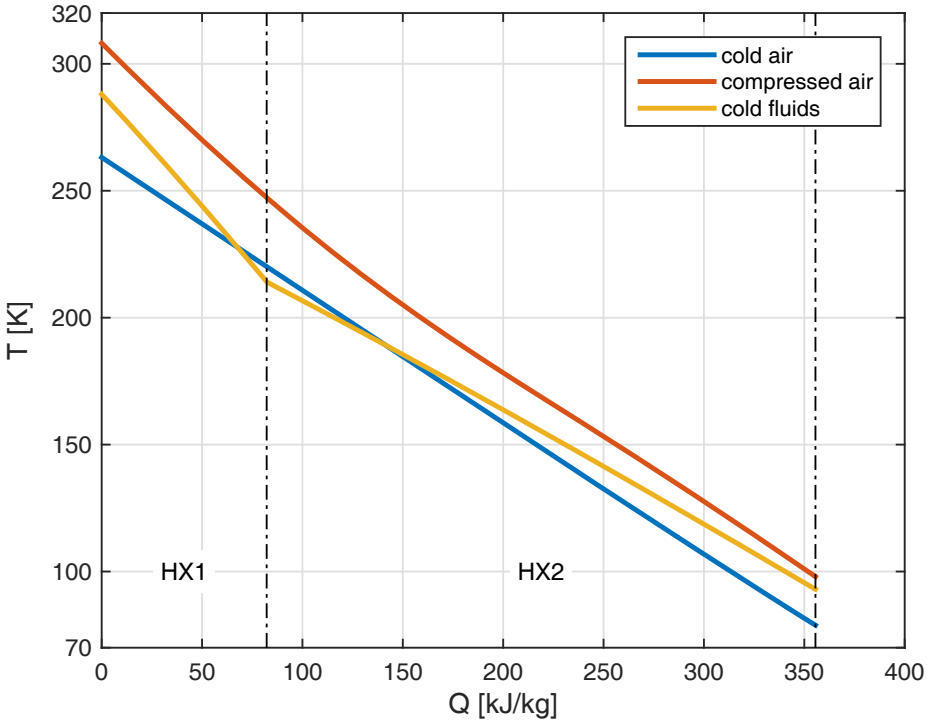

Figure 5: Cold Box heat exchange diagram for $p_{2R} = 6.5\,\mathrm{MPa}$ and $p_2 = 20.0\,\mathrm{MPa}$.

Giuseppe Leo Guizzi, Michele Manno, Ludovica Maria Tolomei, Ruggero Maria Vitali, Thermodynamic analysis of a liquid air energy storage system, Energy 93 (2015) 1639-1647, https://doi.org/10.1016/j.energy.2015.10.030.

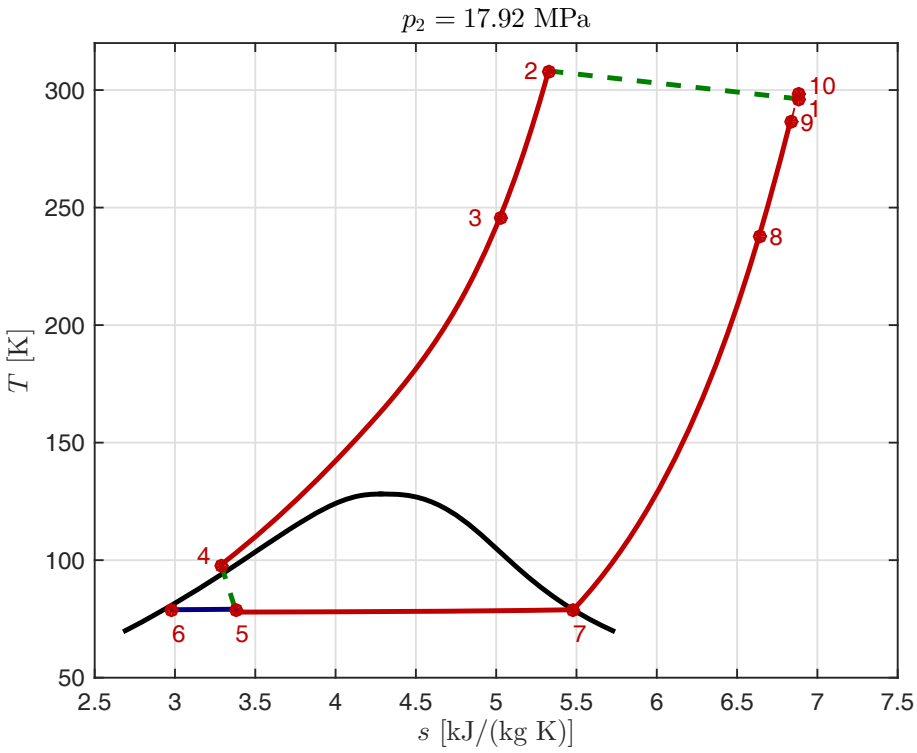

Figure 6: Gibbs plot for the energy storage section.

Giuseppe Leo Guizzi, Michele Manno, Ludovica Maria Tolomei, Ruggero Maria Vitali, Thermodynamic analysis of a liquid air energy storage system, Energy 93 (2015) 1639-1647, https://doi.org/10.1016/j.energy.2015.10.030.

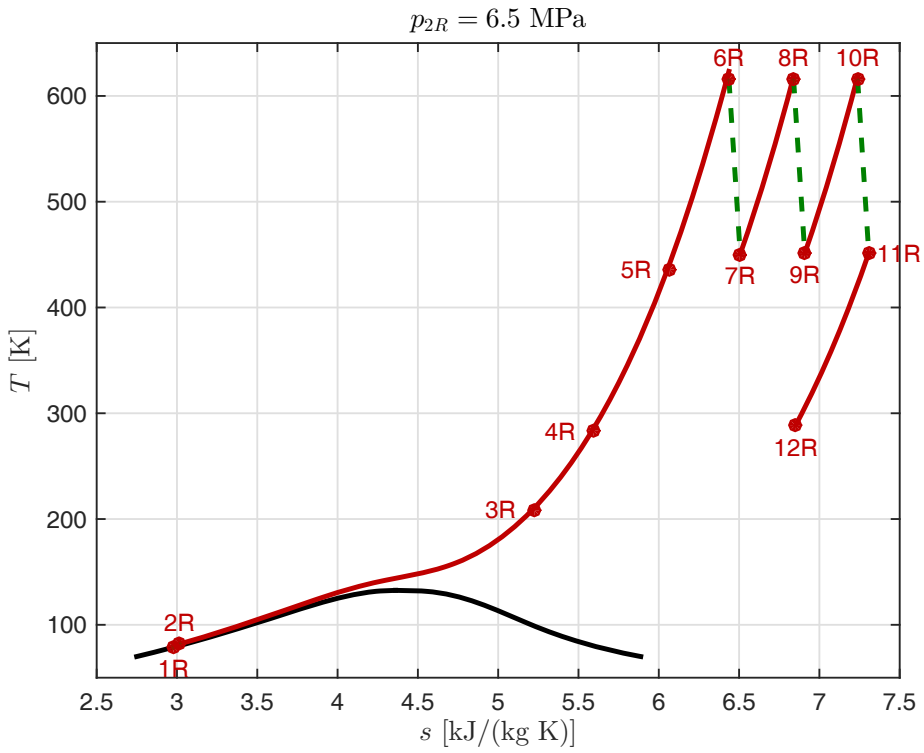

Figure 7: Gibbs plot for the energy recovery section.

Giuseppe Leo Guizzi, Michele Manno, Ludovica Maria Tolomei, Ruggero Maria Vitali, Thermodynamic analysis of a liquid air energy storage system, Energy 93 (2015) 1639-1647, https://doi.org/10.1016/j.energy.2015.10.030.

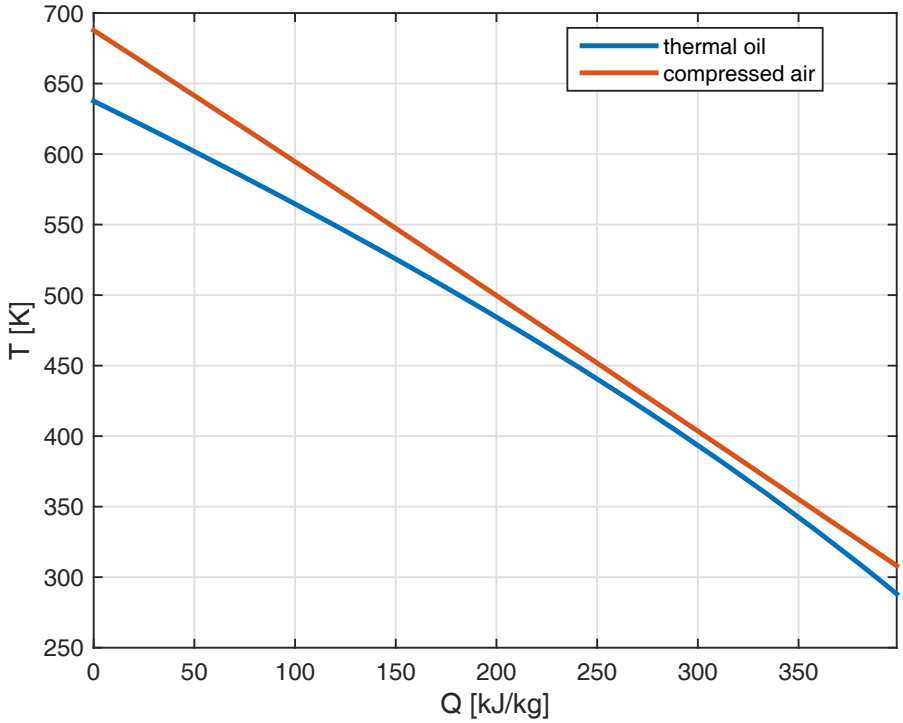

Figure 8: First intercooler heat exchange diagram.

Giuseppe Leo Guizzi, Michele Manno, Ludovica Maria Tolomei, Ruggero Maria Vitali, Thermodynamic analysis of a liquid air energy storage system, Energy 93 (2015) 1639-1647, https://doi.org/10.1016/j.energy.2015.10.030.

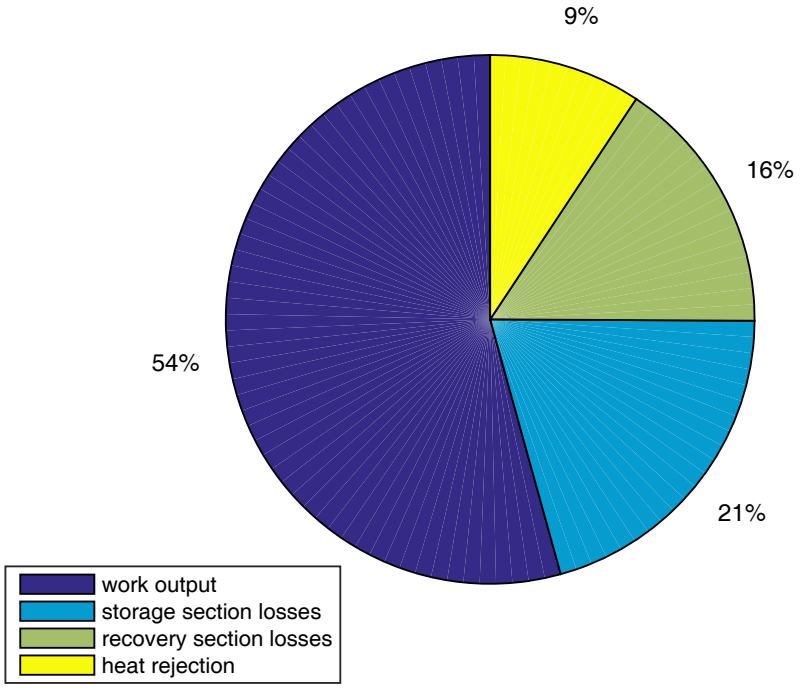

Figure 9: Exergy analysis for the overall LAES plant.

Giuseppe Leo Guizzi, Michele Manno, Ludovica Maria Tolomei, Ruggero Maria Vitali, Thermodynamic analysis of a liquid air energy storage system, Energy 93 (2015) 1639-1647, https://doi.org/10.1016/j.energy.2015.10.030.

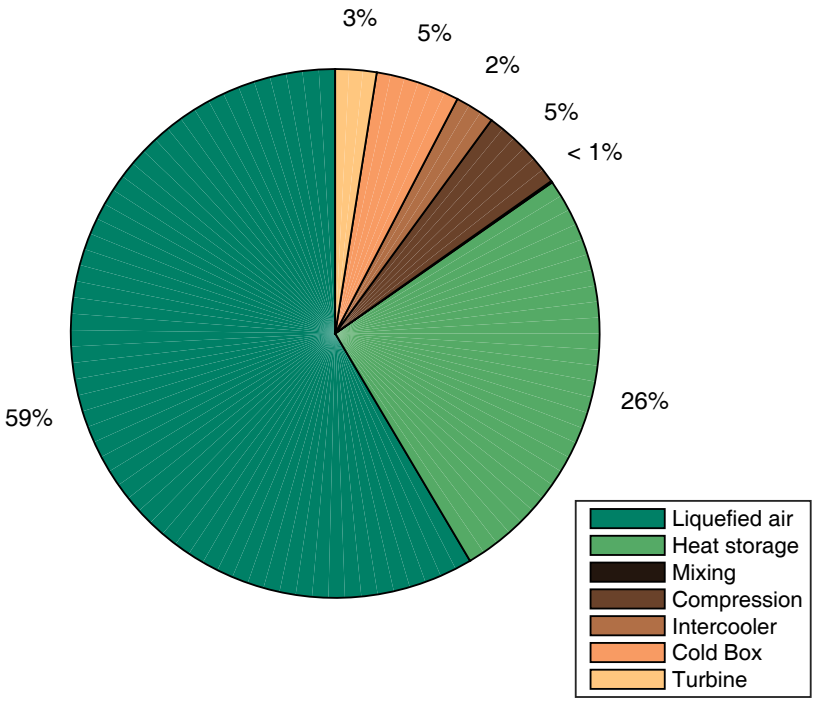

Figure 10: Exergy analysis for the energy storage section; green: exergy outputs; brown: exergy losses.

Giuseppe Leo Guizzi, Michele Manno, Ludovica Maria Tolomei, Ruggero Maria Vitali, Thermodynamic analysis of a liquid air energy storage system, Energy 93 (2015) 1639-1647, https://doi.org/10.1016/j.energy.2015.10.030.

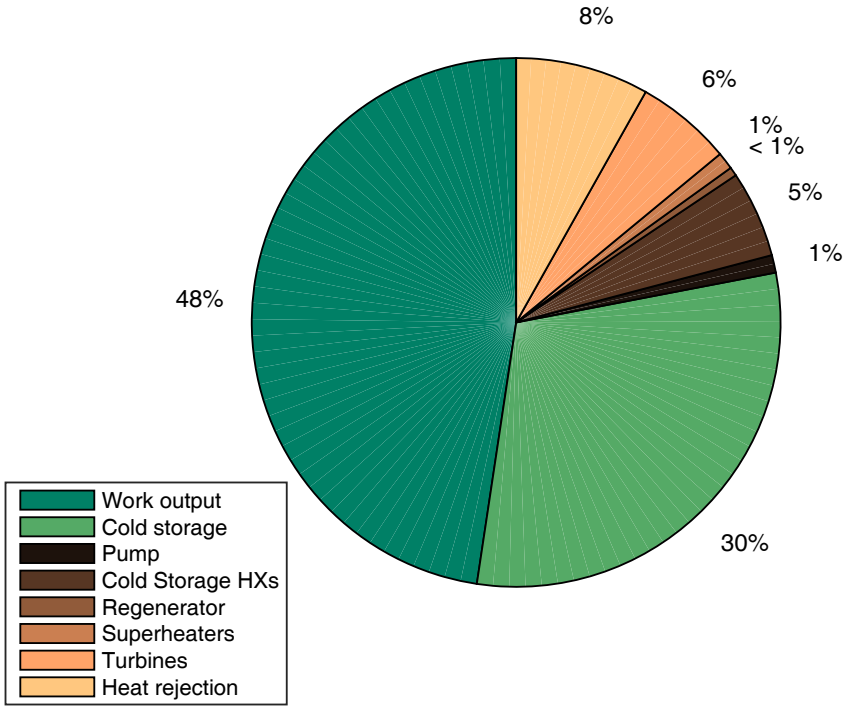

Figure 11: Exergy analysis for the energy recovery section; green: exergy outputs; brown: exergy losses.

Giuseppe Leo Guizzi, Michele Manno, Ludovica Maria Tolomei, Ruggero Maria Vitali, Thermodynamic analysis of a liquid air energy storage system, Energy 93 (2015) 1639-1647, https://doi.org/10.1016/j.energy.2015.10.030.

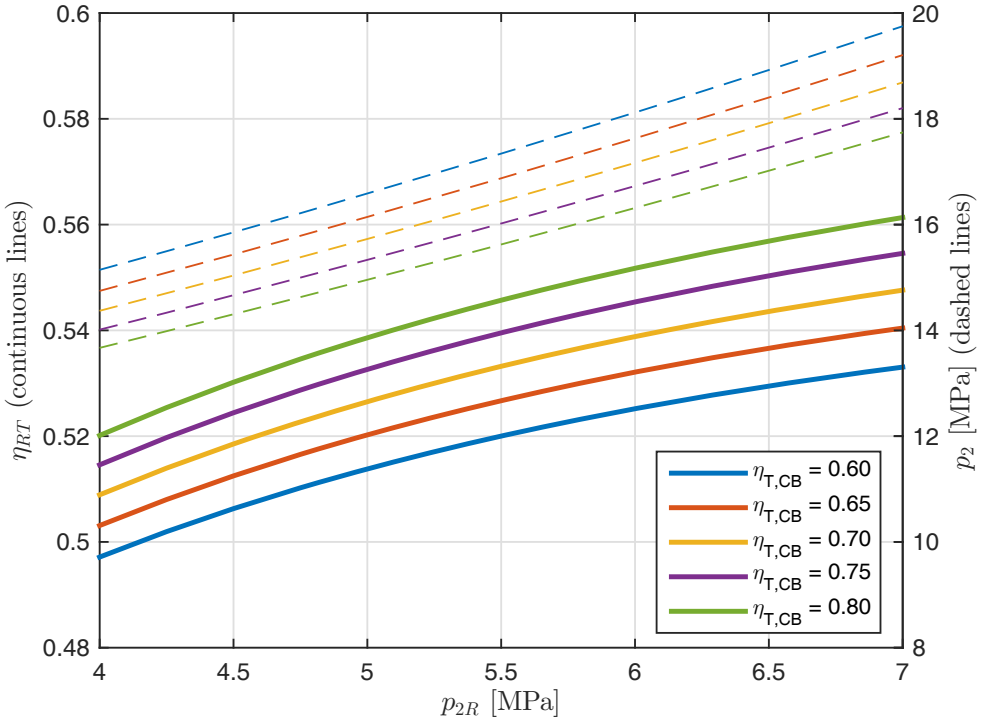

Figure 12: Influence of cryoturbine isentropic efficiency on system's performance.

Giuseppe Leo Guizzi, Michele Manno, Ludovica Maria Tolomei, Ruggero Maria Vitali, Thermodynamic analysis of a liquid air energy storage system, Energy 93 (2015) 1639-1647, https://doi.org/10.1016/j.energy.2015.10.030.

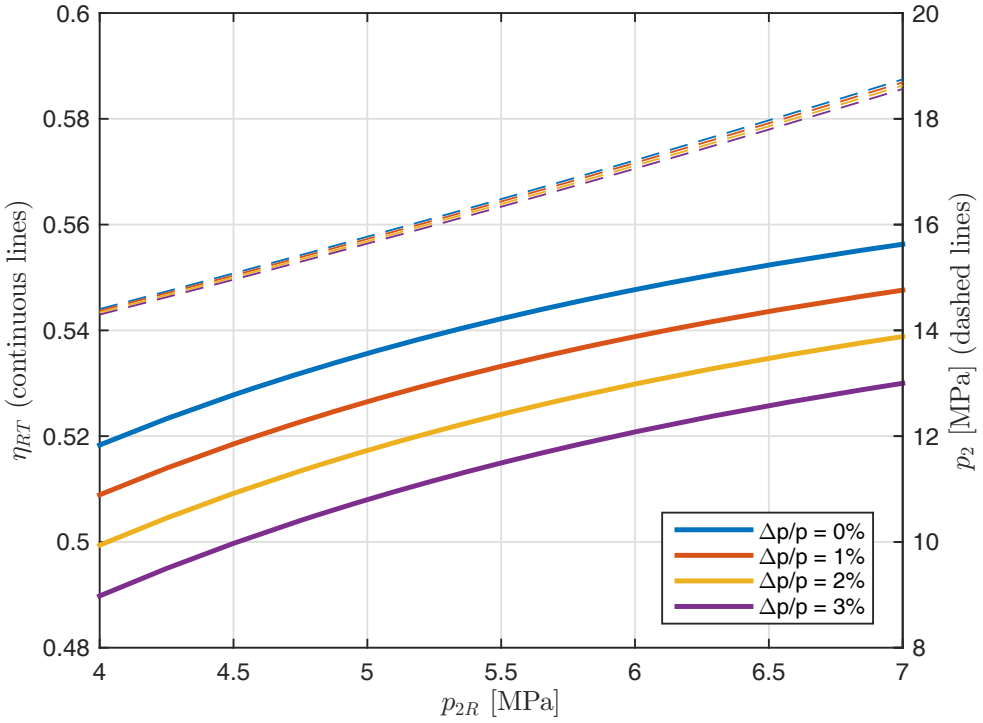

Figure 13: Influence of heat exchangers pressure losses on system's performance.

Giuseppe Leo Guizzi, Michele Manno, Ludovica Maria Tolomei, Ruggero Maria Vitali, Thermodynamic analysis of a liquid air energy storage system, Energy 93 (2015) 1639-1647, https://doi.org/10.1016/j.energy.2015.10.030.

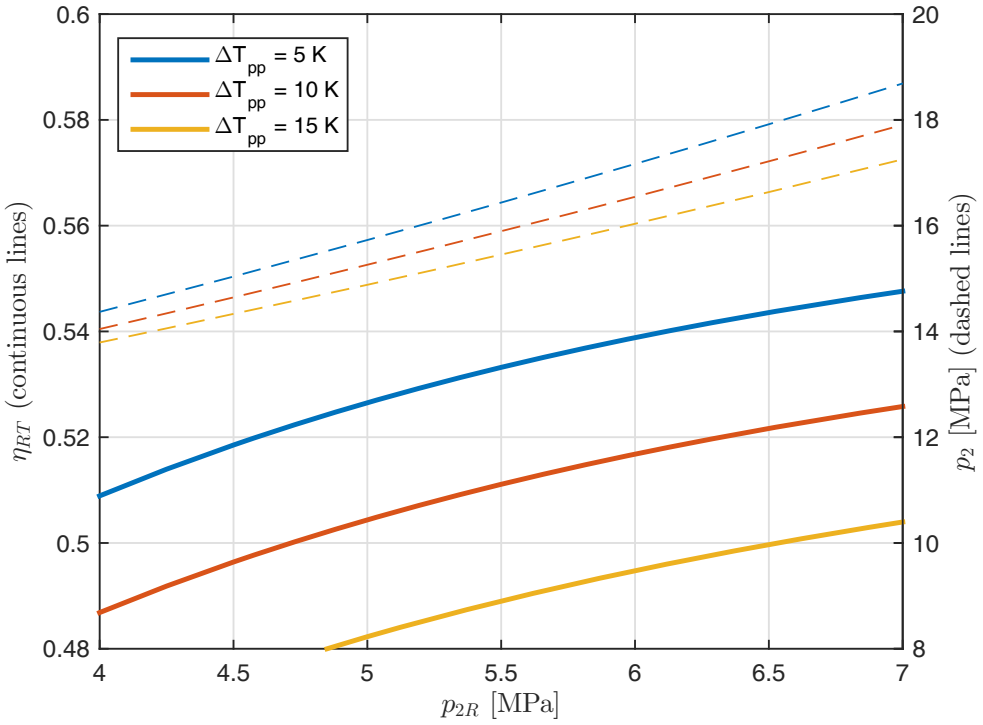

Figure 14: Influence of cold box heat exchanger pinch-point temperature difference on system's performance.

Giuseppe Leo Guizzi, Michele Manno, Ludovica Maria Tolomei, Ruggero Maria Vitali, Thermodynamic analysis of a liquid air energy storage system, Energy 93 (2015) 1639-1647, https://doi.org/10.1016/j.energy.2015.10.030.